NUMERICAL SIMULATIONS OF AN ALTERNATIVE ELASTO-VISCOPLASTIC MODEL

Daniel Dall'Onder dos Santos, dallonder@mecanica.ufrgs.br
Sérgio Frey, frey@mecanica.ufrgs.br
Laboratory of Computational and Applied Fluid Mechanics (LAMAC) – Department of Mechanical Engineering – Universidade Federal do Rio Grande do Sul – Rua Sarmento Leite, 425 – 90050-170 – Porto Alegre, RS, Brazil

Mônica F. Naccache, naccache@puc-rio.br
Paulo Roberto de Souza Mendes, pmendes@puc-rio.br
Department of Mechanical Engineering, Pontifícia Universidade Católica do Rio de Janeiro
Rua Marquês de São Vicente, 225 – 22453-900 – Rio de Janeiro, RJ, Brazil

Abstract. *The main goal of this article is to perform stabilized finite element approximations for inertialess flows of an alternative elasto-viscoplastic model, based on the thixotropic model proposed by de Souza Mendes (2009). This model is approximated by a multi-field Galerkin least squares method in extra-stress, pressure and velocity. This methodology does not need to satisfy the compatibility conditions arisen from finite element sub-spaces for extra-stress–velocity and pressure–velocity. By adding to the classical Galerkin formulation mesh-dependent terms, which are functions of the residuals of the flow governing equations, the stability is obtained without upsetting the classical method consistency. Numerical simulations of the flow over a planar expansion-contraction are carried out. To evaluate the influence of yield stress limit (using for this the flow intensity* U^**), microstructure shear modulus, power law index and jump number,* U^* *is varied from* $7.5x10^{-3}$ *to 1.5,* θ_0^* *from 1.0 to 666.67; n was taken from 0.2 to 0.65 and J from* $5x10^2$ *to* $5x10^4$*, respectively*

Keywords*: elasto-viscoplasticity; structured fluid, regularized viscoplastic models; multi-field Galerkin least-squares method.*

1. INTRODUCTION

Many fluids encountered in industrial processes and applications exhibit non-Newtonian behavior. Some of them are called viscoplastic liquids, once they present a solid-like behavior when the stress level at which they are subject is less then the material yield-stress – common examples are cosmetics, foods, personal care products, paints, cements, drilling muds, crude oil and polymer melts. Thus, the yield stress is known as the most important characteristic of viscoplastic fluids. However, some experimental data demonstrate that elasticity is observed on the apparently unyielded regions formed on viscoplastic fluid flows (Sikorski *et al*., 2009; de Souza Mendes *et al.*, 2007). In this regions, the fluid microstructure is on a stable configuration and, once the stress level at the fluid exceeds the yield stress value, this structure collapses causing a dramatic drop in viscosity and elasticity.

On this work, stabilized finite element approximations are employed to investigate the performance of an alternative model for elasto-viscoplasticity, based on a modification of the viscosity function proposed by de Souza Mendes and Dutra (2004) and on the Oldroyd-B equation for viscoelastic materials. The relaxation time is defined as the relation between the purely viscous response of the material – given by the modified viscosity function – and the microstructure shear modulus, G, function of the steady-state structure parameter which measures the structuring level of the material – see de Souza Mendes (2009) for more details. To approximate this elasto-viscoplastic model, a multi-field Galerkin least squares method in terms of extra-stress, pressure and velocity is employed. This methodology – introduced firstly for the Stokes problem by Hughes *et al.* (1986) – does not need to satisfy the compatibility conditions arisen from the finite element sub-spaces for extra-stress–velocity and pressure–velocity fields once it enhances the stability of the classical Galerkin method adding mesh-dependent terms.

The numerical simulations of the flow over a planar abrupt expansion-contraction are carried out in order to evaluate the influence of the flow intensity, jump number, microstructure shear modulus and power law index on the yield surfaces of elasto-viscoplastic materials. The dimensionless flow-rate U^* is varied from $7.5x10^{-3}$ to 1.5, the non-dimensional relaxation time for the fully structured material, θ_0^*, from 1.0 to 666.67; the power law index was taken from 0.2 to 0.65 and the jump number J from $5x10^2$ to $5x10^4$. For all computations, a combination of equal-order bilinear finite element interpolations are used to approximate the primal variables of the problem, thence violating the involved compatibility conditions. The results obtained in this work are qualitatively in accordance with the related viscoplastic and elasto-viscoplastic literature and proved to be physical meaningful.

2. MECHANICAL MODELING

The relevant equations for a multi-field boundary value problem accounting for isothermal and incompressible fluid flows may be formed by coupling the mass conservation and the momentum balance equations with the upper-convected Maxwell viscoelastic equation. Subjecting the system to he appropriate velocity ans stress boundary conditions, it becomes

$$\begin{aligned}
&\rho(\nabla\mathbf{u})\mathbf{u} = -\nabla p + \operatorname{div}\boldsymbol{\tau} + \mathbf{f} && \text{in } \Omega \\
&\boldsymbol{\tau} + \theta(\dot{\gamma})\overset{\nabla}{\boldsymbol{\tau}} = 2\eta_{ss}(\dot{\gamma})\mathbf{D}(\mathbf{u}) && \text{in } \Omega \\
&\operatorname{div}\mathbf{u} = 0 && \text{in } \Omega \\
&\mathbf{u} = \mathbf{u}_g && \text{on } \Gamma_g^{\mathbf{u}} \\
&\boldsymbol{\tau} = \boldsymbol{\tau}_g && \text{on } \Gamma_g^{\boldsymbol{\tau}} \\
&[\boldsymbol{\tau} - p\,\mathbf{1}]\mathbf{n} = \mathbf{t}_h && \text{on } \Gamma_h
\end{aligned} \tag{1}$$

where ρ is the fluid density, $\mathbf{u}$ is the velocity vector, $\boldsymbol{\tau}$ the extra-stress tensor, $\mathbf{D}$ is the strain rate tensor, p the hydrostatic pressure, $\mathbf{f}$ is the body force vector, η_{ss} and θ are, respectively, the viscosity and the relaxation time of the fluid – functions of the second invariant of $\mathbf{D}$; $\mathbf{t}_h$ is the stress vector, $\mathbf{u}_g$ and $\boldsymbol{\tau}_g$ are the imposed velocity and extra-stress boundary conditions, respectively, and $\overset{\nabla}{\boldsymbol{\tau}}$ stands for the upper-convected time derivative of $\boldsymbol{\tau}$, given by

$$\overset{\nabla}{\boldsymbol{\tau}} = (\nabla\boldsymbol{\tau})\mathbf{u} - (\nabla\mathbf{u})\boldsymbol{\tau} - \boldsymbol{\tau}(\nabla\mathbf{u}^T) \tag{2}$$

In this work, the elasto-viscoplastic constitutive equation employed is based on a modification of the viscosity function proposed by de Souza Mendes and Dutra (2004) and on the Oldroyd-B equation for viscoelastic materials – Eq. (1b). The steady-state viscosity function is given by

$$\eta_{ss}(\dot{\gamma}) = \left(1 - \exp\left(-\frac{\eta_0\,\dot{\gamma}}{\tau_0}\right)\right)\left(\frac{\tau_0 - \tau_{0d}}{\dot{\gamma}}\exp\left(-\frac{\dot{\gamma}}{\dot{\gamma}_0}\right) + \frac{\tau_{0d}}{\dot{\gamma}} + K\,\dot{\gamma}^{n-1}\right) + \eta_\infty \tag{3}$$

where η_0 is the viscosity of the completely structured material, η_∞ is the viscosity of the completely unstructured material, τ_0 is the static yield stress, τ_{0d} is the dynamic yield stress, $\dot{\gamma}_{0d}$ is the shear rate that marks the transition in the stress from τ_0 to τ_{0d}, K is the consistency index and n the power-law index – see, for more details, de Souza Mendes (2009).

The relaxation time θ is defined as the relation between the purely viscous response of the material – given by the viscosity function on Eq. (3) – and the microstructure shear modulus G,

$$\theta(\dot{\gamma}) = \frac{\eta(\dot{\gamma})}{G(\lambda_{ss}(\dot{\gamma}))} \tag{4}$$

The expression employed to evaluate the microstructure shear modulus takes into account the steady-state structure parameter λ_{ss}, which measures the structuring level of the material and is also a function of the strain rate. $G(\lambda_{ss}(\dot{\gamma}))$ should be small when the fluid is fully structured $(\lambda_{ss} = 1)$ and, on the limit where the structure is completely destroyed $(\lambda_{ss} = 0)$, should be infinite to suppress the elastic therm on Eq. (1b) – describing a purely viscous behavior. Thus, the employed expression for the microstructure shear modulus is

$$G = \frac{G_0}{\lambda_{ss}^m} \tag{5}$$

where G_0 is the shear modulus of the completely structured material, m is a positive dimensionless constant and

$$\lambda_{ss}(\dot{\gamma}) = \left(\frac{\ln\eta_{ss}(\dot{\gamma}) - \ln\eta_\infty}{\ln\eta_0 - \ln\eta_\infty}\right) \tag{6}$$

3. FINITE ELEMENT APPROXIMATION

Based on the usual definitions for the finite element subspaces for extra stress ($\boldsymbol{\Sigma}^h$), velocity ($\mathbf{V}^h$) and pressure (P^h) fields (Behr *et al*, 1993), a multi-field Galerkin least-squares formulation for elasto-viscoplastic fluid flows may be

written as: given the functions of body force **f** and Dirichlet and Neumann boundary conditions $\boldsymbol{\tau}_g$ and $\mathbf{u}_g$, and $\mathbf{t}_h$ respectively, find the triple $(\boldsymbol{\tau}^h, p^h, \mathbf{u}^h) \in \boldsymbol{\Sigma}^h \times P^h \times \mathbf{V}_g{}^h$ such that

$$B(\boldsymbol{\tau}^h, p^h, \mathbf{u}^h; \mathbf{S}^h, q^h, \mathbf{v}^h) = F(\mathbf{S}^h, q^h, \mathbf{v}^h) \qquad \forall (\mathbf{S}^h, q^h, \mathbf{v}^h) \in \boldsymbol{\Sigma}^h \times P^h \times \mathbf{V}_g^h \tag{7}$$

with

$$\begin{aligned}
&B(\boldsymbol{\tau}^h, p^h, \mathbf{u}^h; \mathbf{S}^h, q^h, \mathbf{v}^h) = \int_\Omega \rho([\nabla \mathbf{u}^h]\mathbf{u}^h)\cdot \mathbf{v}^h d\Omega + \int_\Omega \boldsymbol{\tau}^h \cdot \mathbf{D}(\mathbf{v}^h) d\Omega - \int_\Omega p^h \operatorname{div} \mathbf{v}^h d\Omega \\
&+ \frac{1}{2\eta_{ss}} \int_\Omega \boldsymbol{\tau}^h \cdot \mathbf{S}^h d\Omega + \frac{1}{2\eta_{ss}} \int_\Omega \theta([\nabla \boldsymbol{\tau}^h]\mathbf{u}^h - [\nabla \mathbf{u}^h]\boldsymbol{\tau}^h - \boldsymbol{\tau}^h[\nabla \mathbf{u}^h]^T)\cdot \mathbf{S}^h d\Omega - \int_\Omega \mathbf{D}(\mathbf{u}^h)\cdot \mathbf{S}^h d\Omega \\
&+ \int_\Omega \operatorname{div} \mathbf{u}^h q^h d\Omega + \epsilon \int_\Omega p^h q^h d\Omega + \delta \int_\Omega \operatorname{div} \mathbf{v}^h \operatorname{div} \mathbf{u}^h d\Omega \\
&+ \sum_{K \in \Omega^h} \int_{\Omega_K} (\rho[\nabla \mathbf{u}^h]\mathbf{u}^h + \nabla p^h - \operatorname{div} \boldsymbol{\tau}^h)\cdot \alpha(Re_{r_K})(\rho[\nabla \mathbf{v}^h]\mathbf{u}^h + \nabla q^h - \operatorname{div} \mathbf{S}^h) d\Omega \\
&+ 2\eta_{ss}\beta \int_\Omega \left(\frac{1}{2\eta_{ss}} \boldsymbol{\tau}^h + \frac{1}{2\eta_{ss}} \theta\big([\nabla \boldsymbol{\tau}^h]\mathbf{u}^h - [\nabla \mathbf{u}^h]\boldsymbol{\tau}^h - [\boldsymbol{\tau}^h](\nabla \mathbf{u}^h)^T\big) - \mathbf{D}(\mathbf{u}^h) \right) \cdot \\
&\qquad \cdot \left(\frac{1}{2\eta_{ss}} \mathbf{S}^h + \frac{1}{2\eta_{ss}} \theta\big([\nabla \mathbf{S}^h]\mathbf{u}^h - [\nabla \mathbf{u}^h]\mathbf{S}^h - [\mathbf{S}^h](\nabla \mathbf{u}^h)^T\big) - \mathbf{D}(\mathbf{v}^h) \right) d\Omega
\end{aligned} \tag{8}$$

and

$$F(\mathbf{S}^h, q^h, \mathbf{v}^h) = \int_\Omega \mathbf{f}\cdot \mathbf{v}^h d\Omega + \int_{\Gamma_h} \mathbf{t}_h \cdot \mathbf{v}^h d\Gamma + \sum_{K \in \Omega^h} \int_{\Omega_K} \mathbf{f}\cdot(\alpha(Re_K)(\rho[\nabla \mathbf{v}^h]\mathbf{u}^h + \nabla q^h - \operatorname{div} \mathbf{S}^h)) d\Omega \tag{9}$$

The grid Reynolds number Re_K and the stability parameters $\alpha(Re_K)$ and δ are defined as

$$\begin{aligned}
&\alpha(Re_K) = \frac{h_K}{2|\mathbf{u}^h|_p} \xi(Re_K) \\
&\xi(Re_K) = \begin{Bmatrix} \mathrm{Re}_K, & 0 < Re_K < 1 \\ 1, & \mathrm{Re}_K > 1 \end{Bmatrix} \\
&Re_K = \frac{\rho h_K |\mathbf{u}^h|_p m_k}{4\eta_{ss}} \\
&m_k = \min\{1/3, 2C_k\}
\end{aligned} \tag{10}$$

where m_k is a positive scalar that takes in to account the the k-degree of the polynomial interpolations; the stability parameter β, which stabilizes the the material equation, is defined as an arbitrary positive value – for more details, see Franca and Frey (1992) and Behr *et al*. (1993).

4. NUMERICAL RESULTS

In this section, the numerical results obtained employing the GLS formulation defined by Eq. (7)-(10) for elasto-viscoplastic fluids flowing through a planar expansion-contraction are presented. The dimensionless parameters employed to characterize the flows – for more details, see Souza Mendes (2007) – are, firstly, the dimensionless flow rate U^*,

$$U^* = \frac{u_0}{\dot{\gamma}_1 h} \tag{11}$$

where u_0 is the flow rate at the channel inlet, h is the characteristic length, taken as half of the entrance channel height, and $\dot{\gamma}_1$ is defined as the strain rate where the fluid begins to flow as a power-law one. The viscosity jump when the stress is around the yield stress value is measured by the jump number J, and is written as

$$J = \frac{\eta_0 \dot{\gamma}_1}{\tau_0} - 1 \tag{13}$$

To quantify the elastic effects at the flow, its employed the non-dimensional relaxation time for the fully structured material, which relates the viscosity jump measured by the *jump number* with the microstructure shear modulus,

$$\theta_0^* = \frac{\tau_0}{G_0}(J+1) \tag{14}$$

To account the inertia effects, the dimensionless density ρ^* can be employed – although only inertialess results are show in this work – and is defined as

$$\rho^* = \frac{\rho(\dot{\gamma}_1 h)^2}{\tau_{0d}} \tag{12}$$

Figure 1 shows a sketch of the studied geometry, a planar channel with a sudden expansion followed by a contraction. The boundary conditions employed in the numerical simulations are uniform parallel velocity u_0 at channel inlet and outlet, no-slip and impermeability on channel walls and symmetry conditions on the channel centerline ($\partial_2 u_1 = u_2 = \tau_{12} = 0$). The expansion-contraction aspect ratios on height (H/h) and width (L/h) are set as 6.3. In order to guarantee fully-developed flow regions upstream and downstream channels, the mesh lengths either upstream or downstream of the expansion-contraction set equal to $20h$. After a mesh independence procedure that compares the transversal dimensionless stress profile at the expansion-contraction center for each consecutive mesh refinement, the selected mesh, with 5,200 bilinear Lagrangian (Q1) finite elements, presents an overall error less then 1% when compared to the next more refined mesh. It's important mentioning that in all the simulations performed in this work, $\rho^*=0.0$, $\eta_\infty \dot{\gamma}_1/\tau_{0d} = 10^{-2}$, $\dot{\gamma}_{0d}/\dot{\gamma}_1 = 10^{-4}$, $\tau_0/\tau_{0d} = 2$ and $m=0.1$.

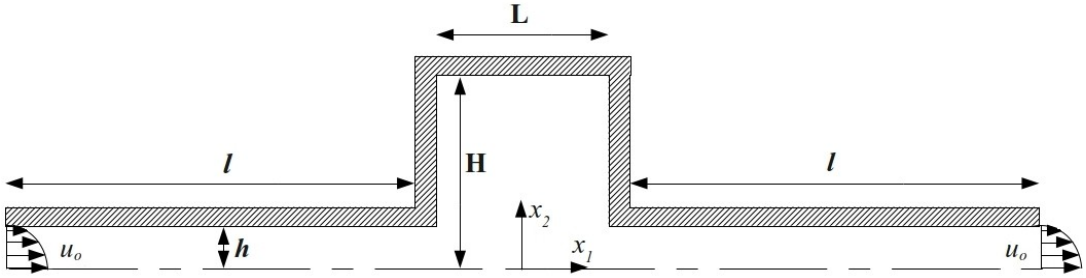

Figure 1. Flow over an expansion-contraction – the problem statement.

The influence of the shear modulus of the completely structured material (G_0) on the unyielded surfaces of the material and on the viscosity and relaxation time isobands is shown, respectively, on Fig 2 and 3, for, $J=5000$, $n=0.5$ and $U^*=0.1$. For high values of the shear modulus, the unyielded regions are almost symmetric – the same trend observed on the viscosity and relaxation time isobands. With the decrease of the shear modulus, the fields became asymmetric due to the increase of the elastic effects on the flow – see, for some qualitative experimental comparison, de Souza Mendes *et al*, 2007.

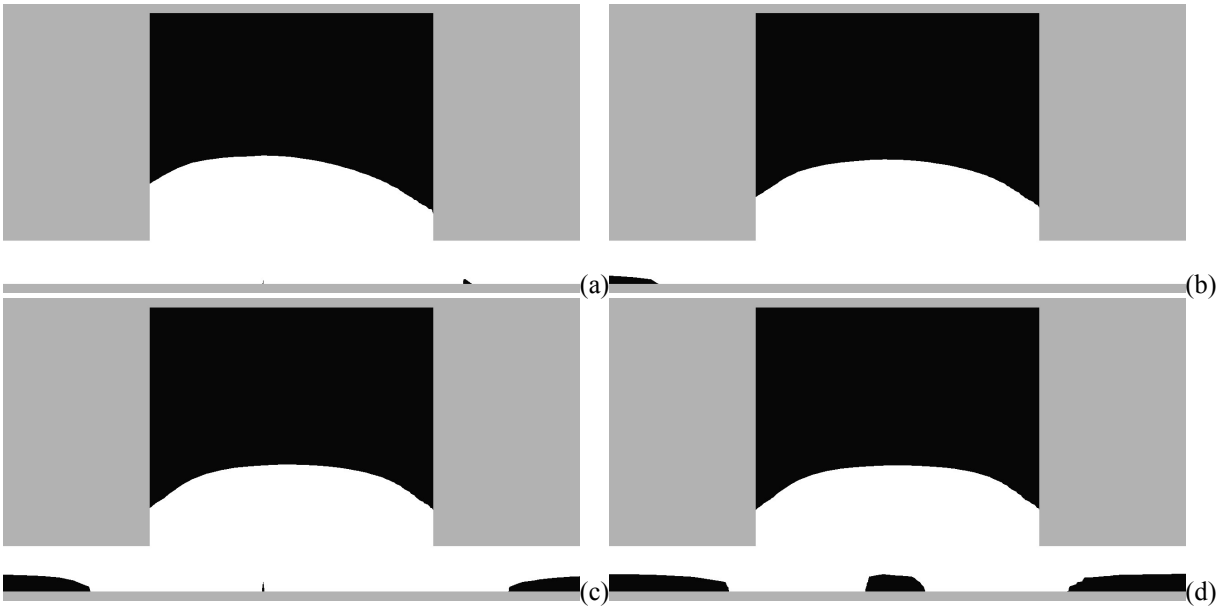

Figure 2. Yielded and unyielded regions, for $J=5000$, $n=0.5$ and $U^*=0.1$: (a) $\theta_0^*=666.67$; (b) $\theta_0^*=200$; (c) $\theta_0^*=40$; (d) $\theta_0^*=1.0$.

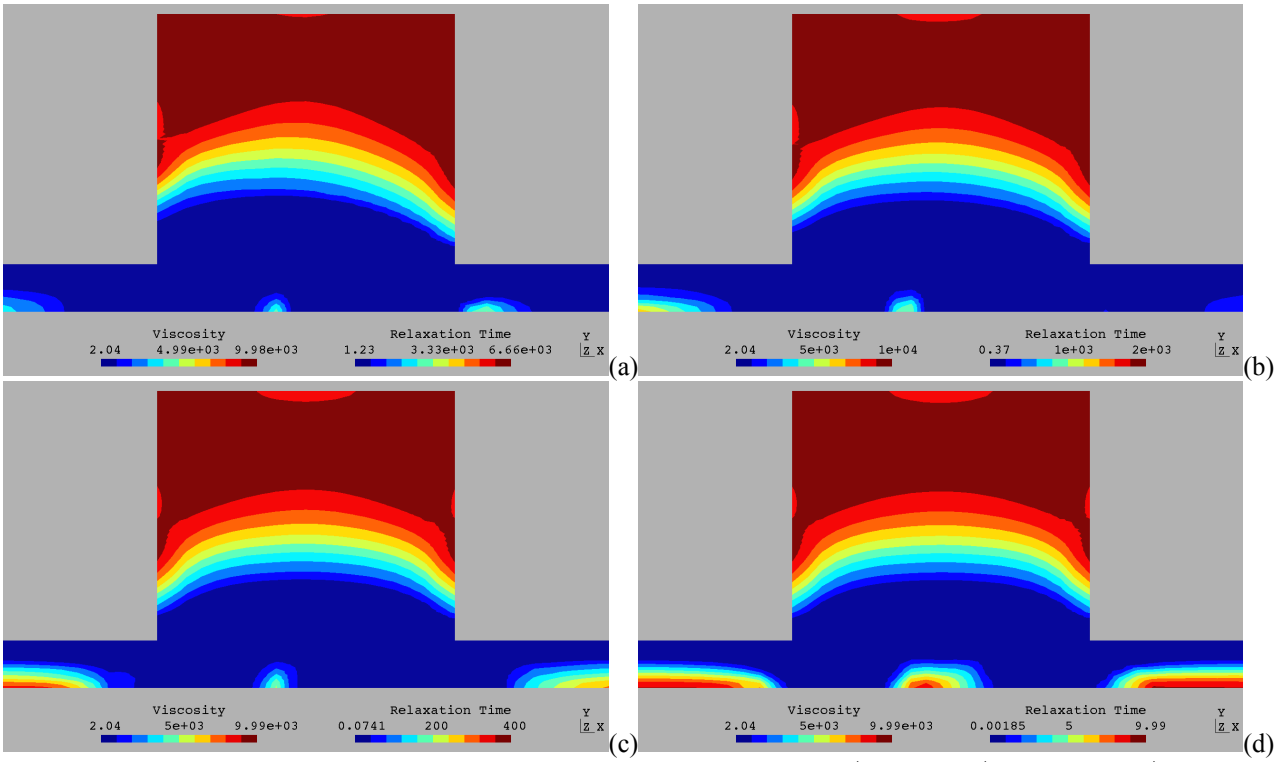

Figure 3. Viscosity and relaxation time isobands, for J=5000, n=0.5 and U^*=0.1: (a) θ_0^*=666.67; (b) θ_0^*=200; (c) θ_0^*=40; (d) θ_0^*=1.0.

Figure 4 shows the effects of the increasing of the flow intensity U^* on the unyielded regions of the flow, for J=5000, n=0.5 and θ_0^*=666.67. Even for the lowest presented value of U^*, the unyielded regions are affected by the elasticity of the material – no symmetry is observed. Increasing the flow intensity, the unyielded regions at the channels are strongly reduced while, inside the cavity, the unyielded regions becomes more asymmetric.

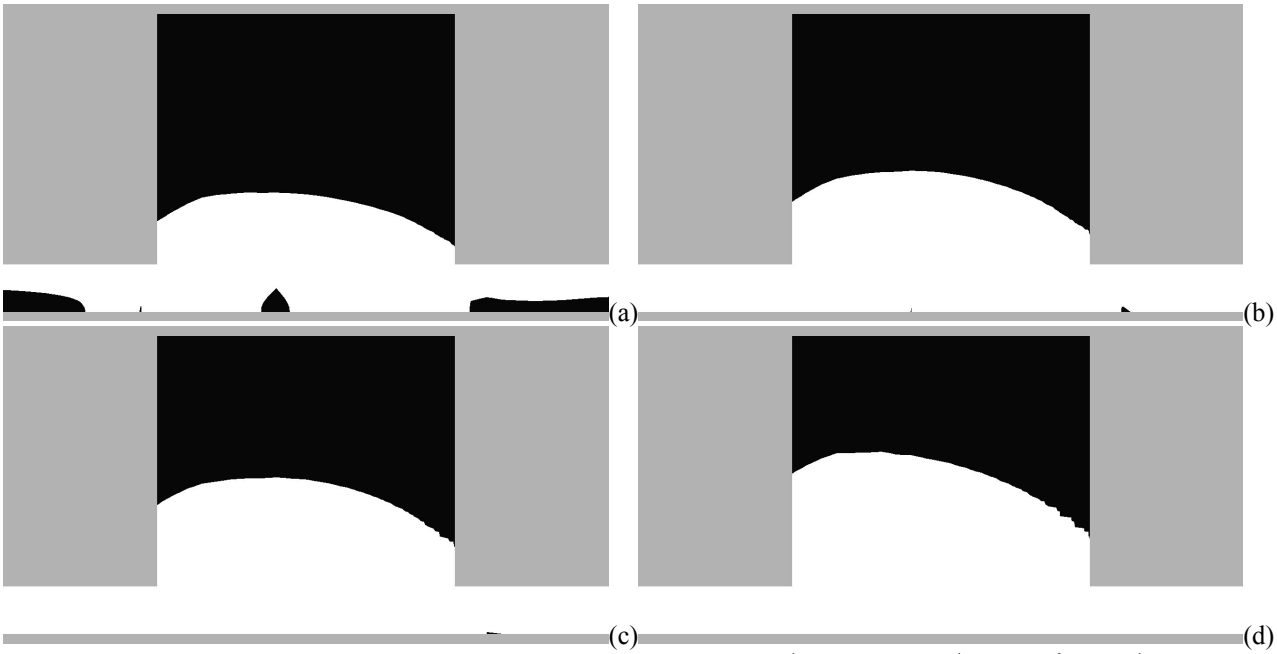

Figure 4. Yielded and unyielded regions, for J=5000, n=0.5 and θ_0^*=666.67: (a) U^*=7.5x10^{-3}; (b) U^*=0.1; (c) U^*=0.4; (d) U^*=1.5.

On Fig. 5 is shown the regularization parameter influence on the morphology of the flow unyielded regions. From Eq. (3), it can be observed that the viscosity equation is regularized by the therm $(1-\exp(-\eta_0\dot{\gamma}/\tau_0))$, making the expression tends to the viscosity of the completely structured material (η_0) when the strain rate tends to very low values.

Thus, to assess the influence of the regularization, the dimensionless quantity J was ranged from $5x10^2$ to $5x10^4$. The trend presented on the figures is in accordance with Liu *et al.* (2002), where the unyielded regions decrease in size with increasing the regularization parameter and at the contour a zig-zag pattern is observed – this behavior due to the round-off errors associated with the high values of the regularization parameter.

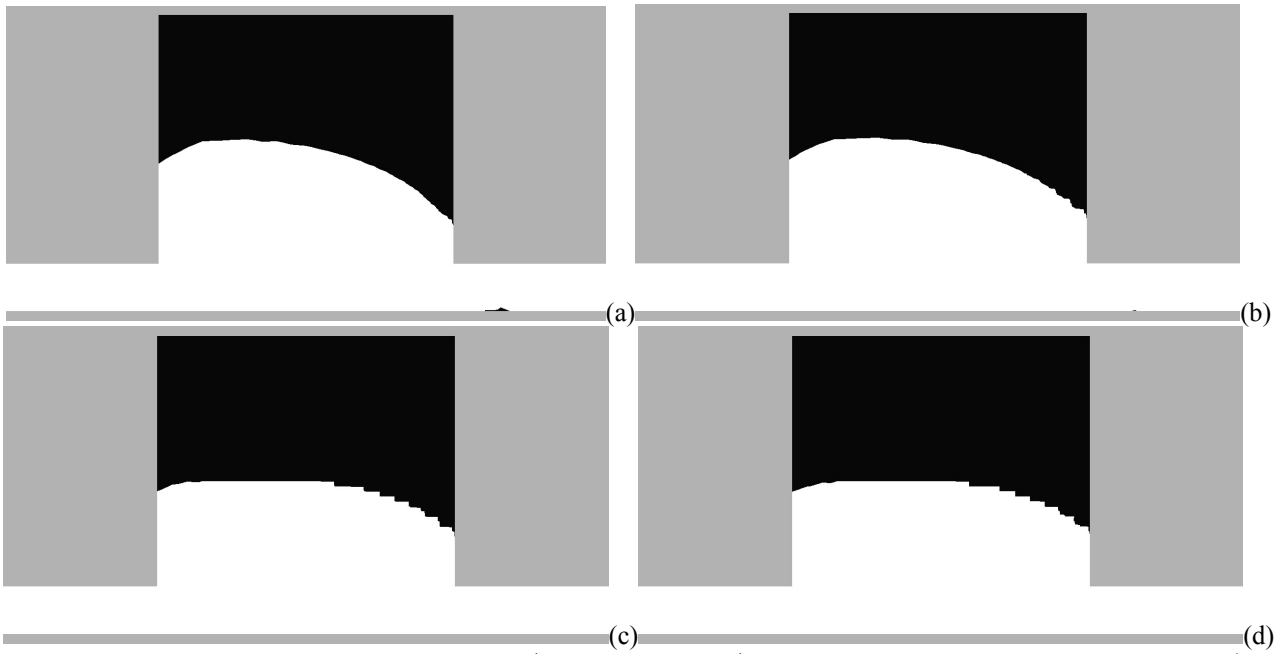

Figure 5. Yielded and unyielded regions, for U^*=1.0, n=0.5 and θ_0^*=666.67: (a) J=500; (b) J=5000; (c) J=2.5x10^4; (d) J=5x10^4.

On the Fig. 8 it can be observed the influence of the power-law index on the flow unyielded regions, for J=5000, U^*=1.0 and θ_0^*=666.67. As n is increased, the trend observed is to symmetrize the unyielded zones at the top of the expansion-contraction. As pointed out in de Souza Mendes *et al.* (2007), the shear-thinning liquids are displaced more easily than Bingham-like viscoplastic liquids (higher n indexes), because shear thinning tends to cause larger deformation rates. This behavior, generates also higher stresses, which amplify the elastic effects and turns the flow more asymmetric.

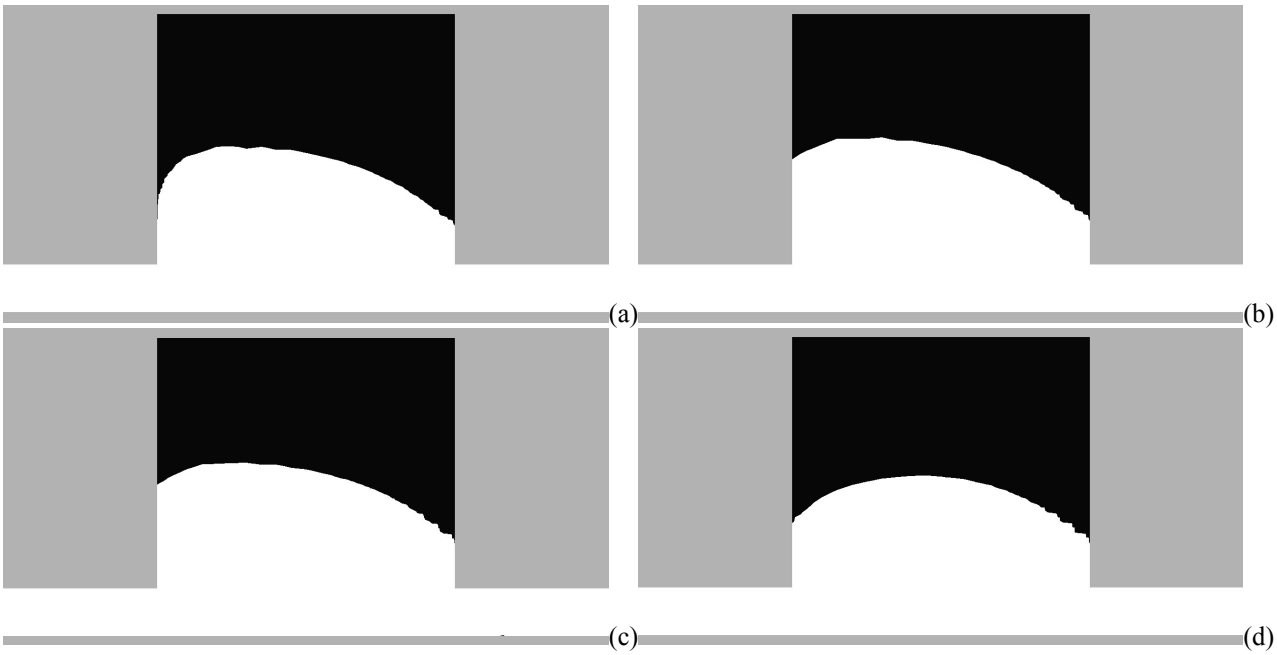

Figure 6. Viscosity and relaxation time isobands, for J=5000, U^*=1.0 and θ_0^*=666.67: (a) n=0.20; (b) n=0.3; (c) n=0.5; (d) n=0.65.

5. FINAL REMARKS

In this article, some numerical simulations of inertialess flows of elasto-viscoplastic fluids have been undertook. The elasto-viscoplastic model was based on the thixotropic model introduced by de Souza Mendes (2009) and the mechanical model was approximated via a multi-field Galerkin least-squares method in extra-stress, pressure and velocity. Due to the good stability features of the GLS method, all computations have employed a combination of equal-order bilinear Lagrangian finite elements and high elastic flows have been stably achieved. The numerical results have evidenced the strong influence of the microstructure shear modulus on the size and position of the unyielded material regions. Also the yield stress level – variated via the flow intensity U^* – proved to play a relevant role on the characterization of the unyielded zones.

6. ACKNOWLEDGEMENTS

The authors D.D.O. Santos thanks the agency CAPES for his graduate scholarship and the authors S. Frey, M.F. Naccache and P.R. de Souza Mendes thanks CNPq and Petrobras for financial support.

7. REFERENCES

Behr, M., Franca, L.P. and Tezduyar, T.E., 1993, "Stabilized Finite Element Methods for the Velocity-Pressure-Stress Formulation of Incompressible Flows", Comput. Methods Appl. Mech. Engrg., Vol. 104, pp. 31-48.

de Souza Mendes, P.R., and Dutra, E.S.S., 2004, "Viscosity Function for Yield-Stress Liquids", Applied Rheology, Vol. 14, pp. 296-302.

de Souza Mendes, P.R., 2007, "Dimensionless non-Newtonian fluid mechanics", J. Non-Newt. Fluid Mech., Vol. 147, pp. 109-116.

de Souza Mendes, P. R., Naccache, M. F., Varges, P. R., and Marchesini, F. H., 2007, "Flow of viscoplastic liquids through axisymmetric expansions-contractions", J. Non-Newt. Fluid Mech., Vol. 142, pp. 207-217.

de Souza Mendes, P.R., 2009, "Modeling the thixotropic behavior of structured fluids", J. Non-Newt. Fluid Mech., Vol. 164, pp. 66-75.

Franca, L.P., and Frey, S., 1992, "Stabilized Finite Element Methods: II. The Incompressible Navier-Stokes Equations", Comput. Methods Appl. Mech. Eng., Vol. 99, pp. 209-233.

Hughes, T.J.R., Franca, L.P., and Balestra, M., 1986, "A new finite element formulation for computational fluid dynamics: V. Circumventing the Babuška-Brezzi condition: A stable Petrov-Galerkin formulation of the Stokes problem accomodating equal-order interpolations", Comput. Methods Appl. Mech. Eng., Vol. 59, pp. 85-99.

Liu, B. T., Muller, S. J., Denn, M. M., 2002, "Convergence of a regularization method for creeping flow of a Bingham material about a rigid sphere", J. Non-Newt. Fluid Mech., Vol. 102, pp. 179-191.

Sikorski, D., Tabuteau, H., de Bruyn, J. R., 2009, "Motion and shape of bubbles rising through a yield-stress fluid", J. Non-Newt. Fluid Mech., Vol. 159, pp. 10-16.

8. RESPONSIBILITY NOTICE

The authors are the only responsible for the printed material included in this paper.